Integrating Spatial Transcriptomics and Imaging Mass Cytometry for Multi-Omic Mapping of Colorectal Liver Metastasis

Merrin Mary Eapen[1,2*], Qanber Raza[3*], Annabel Faulkner[4*], Abhishek Kumar Singh[1], Atefeh Khakpoor[1], Dina Kazemi[1], Erin Coll[2,4,5], Liang Lim[3], Nick Zabinyakov[3], Liang Qiao[6], Anna Di Bartolomeo[6], Jacob George[6], Christina Loh[3], Helen M. McGuire[4], Ankur Sharma[1,2,7]

[1]Garvan Institute of Medical Research, Australia; [2]University of New South Wales, Australia; [3]Standard BioTools Canada Inc., ON, Canada; [4]Faculty of Medicine and Health, University of Sydney, Australia; [5]Children's Cancer Institute, Sydney, Australia; [6]Storr Liver Centre, University of Sydney, Sydney, Australia; [7]KK Women's and Children's Hospital, Singapore

INTRODUCTION

Hepatocellular carcinoma (HCC) is a highly heterogeneous malignancy, requiring spatially resolved multi-omic approaches to advance therapeutic strategies. Spatial transcriptomics using the Xenium platform enables high-throughput mapping of hundreds to thousands of RNA targets within intact tissue architecture. While transcript-level insights provide critical context for understanding gene expression patterns, integrating proteomic data adds a complementary layer that enables direct validation of biomarker expression. Spatial proteomic technologies, such as Imaging Mass Cytometry™ (IMC™), complement transcriptomics by providing high-dimensional protein expression data at subcellular resolution. IMC technology leverages metal-tagged antibodies and laser ablation to simultaneously quantify over 40 protein markers with five orders of magnitude linear dynamic range, surpassing traditional immunohistochemistry and immunofluorescence. Here, we demonstrate the feasibility and biological insights gained from applying IMC technology to same tissue sections previously processed with Xenium, integrating transcriptomic and proteomic data through computational coregistration.

Methods and materials

Colorectal liver metastasis (CRLM) samples from three patients (plus matched adjacent normal liver from one) were processed as FFPE 5 µm sections under ethics approval. For Xenium In Situ, sections were deparaffinized, rehydrated, decrosslinked and hybridized overnight (50 °C) with custom 462- or 319-gene panels, followed by washing, ligation, rolling circle amplification, cell/nuclei staining and imaging on the Xenium Analyzer. For spatial proteomics, sections underwent antigen retrieval (pH 9, 96 °C), BSA blocking and overnight incubation with a validated 43-marker metal-tagged antibody panel, then Ir nuclei staining and acquisition on the Hyperion™ XTi Imaging System. IMC data were segmented/phenotyped in QuPath, and Xenium–IMC datasets were coregistered using DNA/nuclei images via affine transformation.

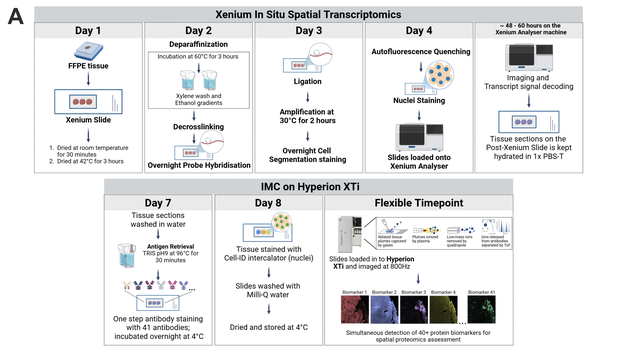

Figure 1. Overview of the integrated spatial multi-omic imaging workflow, panels designed across transcript and protein modalities, and the data analysis workflow. A, Overview of the experimental data generational workflow. FFPE sections from resected tumor specimens were mounted onto Xenium In Situ slides and processed using the 10x Genomics Xenium In Situ hybridization workflow, followed by transcript detection on the Xenium Analyzer. Upon completion of the transcriptomic imaging, the tissue sections underwent antigen retrieval and IMC antibody staining followed by protein co-detection with the Hyperion XTi Imaging System. **B**, Overview of the data analysis approaches as cross-platform DNA identification (DAPI and Cell-ID™) enables data coregistration, joint transcript and protein visualization, and quantitative data analysis.

CONCLUSIONS

Our study describes an integrated spatial multi-omic workflow that sequentially combines Xenium In Situ spatial transcriptomics with IMC spatial proteomics on the Hyperion XTi Imaging System. We demonstrate that:

- Protein epitopes and signal integrity are preserved after Xenium's cyclical chemistry, enabling reliable downstream IMC protein detection with maintained morphology and antigenicity
- Profiling RNA and protein on the same section eliminates the ambiguity of aligning adjacent sections and strengthens single-cell biological inference about state and function
- The approach enables high-fidelity integration so RNA programs can be directly compared with functional protein readouts, including subcellular localization
- This is demonstrated by resolving RNA–protein discordance critical to biology and biomarkers
  - β-catenin localization linked to EMT programs
  - Checkpoint targets where protein is detected more sensitively than transcripts

Results

Sequential Xenium–IMC workflow preserves protein detection

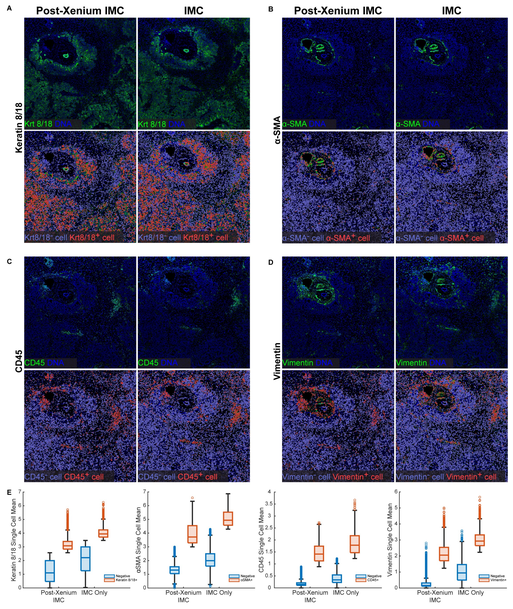

Figure 2. Sequential Xenium–IMC workflow preserves protein detection in CRLM FFPE tissue. Representative IMC images from serial sections of a CRLM ROI show keratin 8/18 (A), αSMA (B), CD45 (C) and vimentin (D) following the sequential spatial multi-omic workflow (Xenium first, then IMC technology) compared with a standard workflow using only IMC technology. QuPath-based single-cell segmentation and marker-positive/negative classification are shown (bottom row). (E) Quantification of mean marker intensity demonstrates comparable signal separation between marker-positive and marker-negative populations, indicating maintained protein sensitivity after the sequential multi-omic workflow.

Integrated single-section spatial multi-omics resolves post-transcriptional regulation of β-catenin

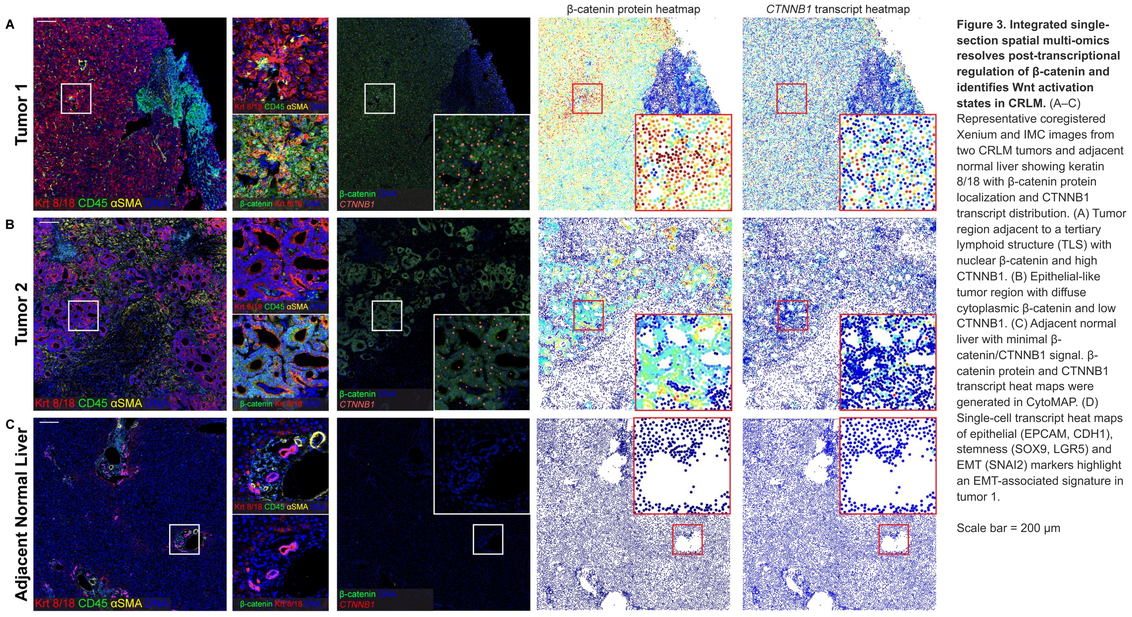

Figure 3. Integrated single-section spatial multi-omics resolves post-transcriptional regulation of β-catenin and identifies Wnt activation states in CRLM. (A–C) Representative coregistered Xenium and IMC images from two CRLM tumors and adjacent normal liver showing keratin 8/18 with β-catenin protein localization and CTNNB1 transcript distribution. (A) Tumor region adjacent to a tertiary lymphoid structure (TLS) with nuclear β-catenin and high CTNNB1. (B) Epithelial-like tumor region with diffuse cytoplasmic β-catenin and low CTNNB1. (C) Adjacent normal liver with minimal β-catenin/CTNNB1 signal. β-catenin protein and CTNNB1 transcript heat maps were generated in CytoMAP. (D) Single-cell transcript heat maps of epithelial (EPCAM, CDH1), stemness (SOX9, LGR5) and EMT (SNAI2) markers highlight an EMT-associated signature in tumor 1.

Scale bar = 200 µm

Multi-omic mapping resolves lymphoid and myeloid cell phenotypes and checkpoint marker expression in tertiary lymphoid structure

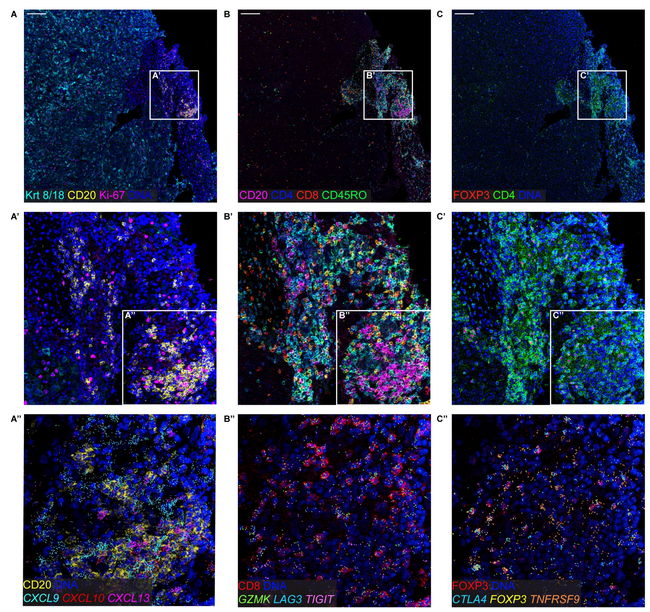

Figure 4. Multi-omic mapping resolves TLS organization and immune activation states in CRLM. (A) IMC technology identifies CD20+ B cell aggregates adjacent to K8/18+ tumor epithelium and proliferating (Ki-67+) lymphocytes within the TLS. (A') Higher-magnification inset highlights B cell cluster architecture and nuclear Ki-67 localization. (A") Coregistered Xenium–IMC data localize chemokine transcripts CXCL9, CXCL10 and CXCL13 to the periphery of B cell aggregates. (B) IMC technology delineates spatial distributions of CD4+ T cells, CD8+ cytotoxic T cells and CD45RO+ memory T cells within the same TLS. (B') Whole-structure view demonstrates coordinated T and B cell compartmentalization. (B") Integrated data identify GZMK+ CD8 T cells and detect co-inhibitory transcripts LAG-3 and TIGIT within the TLS. (C) IMC technology shows distinct CD4 T cell clusters within the TLS and at the tumor interface. (C') FoxP3+ regulatory T cells are localized within the niche. (C") Coregistered transcript/protein maps confirm FoxP3 with CTLA-4 and TNFRSF9 expression in regulatory T cells.

Scale bar = 200 µm

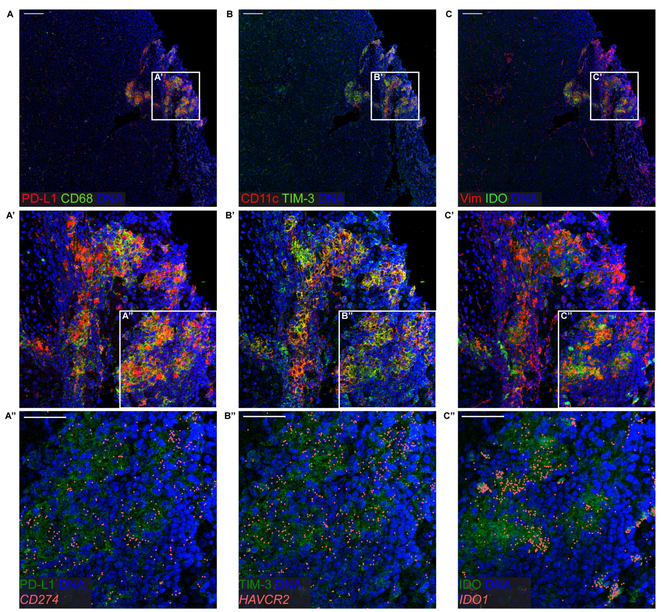

Figure 5. Comprehensive checkpoint immunophenotyping of myeloid niches adjacent to TLS in CRLM reveals RNA–protein detection discrepancies. (A–A') IMC technology shows spatial co-localization of CD68+ macrophages with PD-L1 protein expression near the TLS; (A") coregistered Xenium–IMC workflow visualizes PD-L1 protein with CD274 transcripts. (B–B') IMC technology identifies CD11c+ dendritic cells expressing TIM-3; (B") coregistered data confirm TIM-3 protein with HAVCR2 transcripts. (C–C') IMC technology shows vimentin-rich stromal/immune regions with focal IDO protein expression; (C") coregistered data demonstrate concordant IDO protein with IDO1 transcripts. (D–F) Single-cell protein and transcript heat maps for PD-L1/CD274, TIM-3/HAVCR2 and IDO/IDO1 highlight broader protein detectability relative to transcripts, most pronounced for PD-L1/CD274. Integrating RNA and protein on the same tissue section highlights platform-specific detection limits and reveals cases in which transcripts underestimate protein abundance (for example, PD-L1).

This supports multi-omic profiling to more accurately define immunoregulatory myeloid niches for therapeutic stratification.

Scale bars = 200 µm (A–C) and 50 µm (A"–C")

Standard BioTools Inc.
50 Milk Street, 10th Floor, Boston, MA 02109 US
+1 650 266 6000 • Toll-free in the US and Canada: 866 359 4354
standardbio.com